논문 2010-47CI-1-18

이미지 검색을 위한 Haar 웨이블릿 특징 검출자에 대한 연구

(Study of the Haar Wavelet Feature Detector for Image Retrieval)

팽 소 호*, 김 현 수*, 뮤 잠 멜*, 김 덕 환**

(Shao-Hu Peng, Hyun-Soo Kim, Khairul Muzzammil, and Deok-Hwan Kim)

요 약

본 논문은 Haar 웨이브릿변환과 평균 박스필터에 기반을 둔 Haar 웨이브릿 특징 검출자를 제안한다. 원 영상을 Haar 웨이브릿 변환을 통해 분해하여 영상의 분산정보를 얻고 영상 식별을 위한 특징정보를 추출한다. 영역을 나타내는 주위영역들 중에 분산이 가장 큰 영역의 관심점을 검출하기 위하여 국부 분산정보를 비교하는 평균 박스필터를 적용하고 빠른 계산을 위한 적분영상 기법을 사용한다. Haar 웨이브릿 변환과 평균 박스필터를 이용하여 제안한 검출자는 밝기 변화, 스케일 변화, 영상의 회전에 민감하지 않는 특성을 제공할 수 있다. 실험결과는 제안한 방법이 적은 관심점을 사용하는 경우에도 기존의 DoG 검출자와 Harris corner 검출자에 비해 더 높은 repeatability와 효율성 그리고 매칭정확성을 달성할 수 있음을 보여준다.

Abstract

This paper proposes a Haar Wavelet Feature Detector (HWFD) based on the Haar wavelet transform and average box filter. By decomposing the original image using the Haar wavelet transform, the proposed detector obtains the variance information of the image, making it possible to extract more distinctive features from the original image. For detection of interest points that represent the regions whose variance is the highest among their neighbor regions, we apply the average box filter to evaluate the local variance information and use the integral image technique for fast computation. Due to utilization of the Haar wavelet transform and the average box filter, the proposed detector is robust to illumination change, scale change, and rotation of the image. Experimental results show that even though the proposed method detects fewer interest points, it achieves higher repeatability, higher efficiency and higher matching accuracy compared with the DoG detector and Harris corner detector.

Keywords : Interest point, Haar wavelet, Feature detector, Object recognition

I. Introduction

Object recognition plays a very important role in the domain of artificial intelligence. In recent years, various methods using local features have been used widely for object recognition. These methods detect interest points and extract features from the region around the points in an image for image matching. They have been used in various applications such as medical image processing[1, 4, 24], object categorization [5, 16], image retrieval[11, 19, 23], and object tracking[30~31].

To extract features for image matching, one of the most important steps is to locate the interest points in the image by using effective detectors such as the Harris corner detector[8], DoG detector[14], LoG[17], DoH[18]. The most valuable property of a detector is its repeatability: the higher the repeatability is, the better the detector becomes.

* 학생회원,** 정회원-교신저자, 인하대학교 전자공학과
(Dept of Electronic Engineering, Inha University)

※ 이 논문은 지식경제부와 한국산업기술진흥원의 전략기술인력양성사업의 일환과 2008년도 정부(교육과학기술부)의 재원으로 한국연구재단의 지원을 받아 수행된 연구임(R01-2008-000-20685-0).
접수일자: 2009년10월7일, 수정완료일: 2010년1월11일

Recently, the usefulness of the Scale Invariant Feature Transform (SIFT)[15] for image feature extraction and object recognition has been demonstrated[9, 3]. The DoG detector applied by SIFT achieves high repeatability in situations of involving illumination change, various scales, and rotation. However, the large number of keypoints, ranging from hundreds to thousands, is an inherent problem in applying the DoG detector to image matching and poses a limitation to real time applications.

This paper proposes a Haar Wavelet Feature Detector (HWFD) based on the Haar wavelet transform and the average box filter to detect a small number of interest points with high repeatability and valuable information. Previous detectors such as the Harris corner detector[8], DoG detector[15], and LoG detector[17], aim at either detecting corners or blob regions in the image. In contrast, the proposed detector focuses on detecting interest points, which represent the regions whose variance is the highest among their neighbor regions. Owing to the properties of the Haar wavelet transform, the proposed method is able to obtain the high frequency coefficients of the original image with various scales. Since the high frequency coefficients represent the variance information of the image, they enable extraction of more distinctive features. Furthermore, use of the average box filter and Haar wavelet transform provides robustness to illumination change, scale change, and rotation of the image.

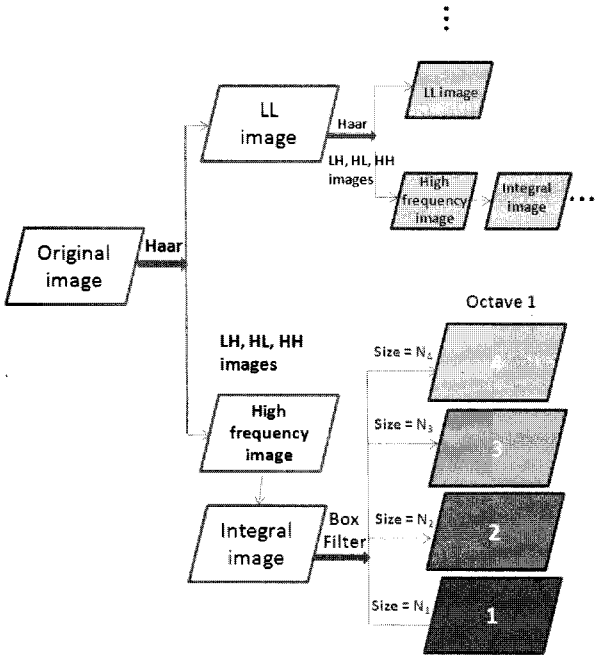

그림 1. 검출자의 주요 과정
Fig. 1. The main process of the detector.

Figure 1 represents the main process of the proposed HWFD method. With the multi-scale and space decomposition properties of the Haar wavelet transform, first, we transform the original image to LH (horizontal direction), HL (vertical direction), and HH (diagonal direction) images. The pixels of these images are composed of high frequency coefficients and they describe the local variance of adjacent pixels of the original image. Second, we fuse these images into a high frequency image and transform the high frequency image into an integral image for fast computation.

Third, to evaluate the variance of the local regions of the original image, we apply the average box filter with various sizes to the integral image. We then build up an octave of an image pyramid that consists of several smoothed images.

By repeating these steps on LL images with different scales, as shown in Figure 1, we can build up the image pyramid with several octaves for a multi-scale analysis. Since the average box filter is applied, a pixel in the smoothed image gives the variance information of the surrounding region. The size of that region corresponds to the size of the box filter. In the next step, we select the points in the smoothed image whose values are larger than an adaptive threshold as candidate points. Finally, we compare the value of the candidate point with those of its neighbors. If the value of the candidate point is the highest, the point is determined to be an interest point.

Since the proposed detector takes advantage of the Haar wavelet transform, it reduces the number of interest points. The interest points detected by the proposed detector are more distinctive and offer

higher repeatability. Thus, the new detector improves the matching accuracy and efficiency in the process of the image matching. Furthermore, due to the application of the integral image technique, the proposed detector achieves fast interest point detection.

In the domain of image retrieval[11, 7, 27, 29], object detection[9, 22], mobile robot systems[20~21], real time processing, computer aided diagnosis are important applications. Since the proposed detector can detect the interest points with fast speed and reduce the number of interest points without degrading its performance, it can be well applied in these applications.

The remainder of this paper is organized as follows: we present the relative works in section II and introduce the proposed detector in section III. In section IV, we describe our experiment. Finally, conclusions are presented in section V.

II. Related Works

The SIFT algorithm includes the following four stages: (1) scale-space extrema point detection; (2) keypoint localization; (3) orientation assignment; and (4) keypoint descriptor[15].

In the first stage, the image is first smoothed by a Gaussian function with different scales and down-sampled to build a Gaussian pyramid. Figure 2 shows the process of building the Gaussian pyramid. A Difference-of-Gaussian (DoG) pyramid is then built by subtracting the adjacent smoothed images in the same octave. Finally, the value of each point in the DoG image is compared with the value of other points around it. If its value is the maximum or the minimum, then it is determined to be a keypoint.

In the second stage, either a keypoint with low contrast or a keypoint close to the edge in the image is pruned for obtaining a stable keypoint.

In the third stage, one or more consistent orientations are assigned for the keypoint in order to achieve invariance of the image rotation.

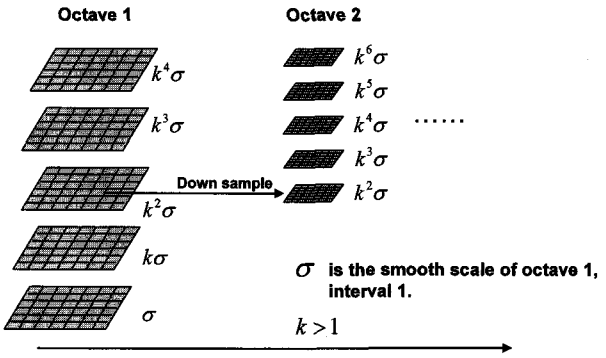

그림 2. 가우시안 피라미드 구성 과정
Fig. 2. The process of building the Gaussian pyramid.

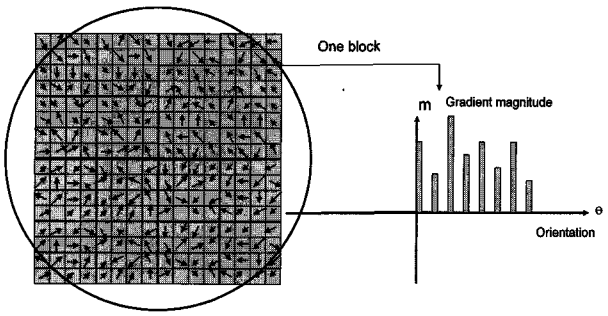

그림 3. 서술자 계산 과정
Fig. 3. The descriptor calculation process.

In the fourth stage, the descriptor is calculated in the region around the keypoint. The region is separated into 16 blocks. The gradient magnitude and the orientation for each pixel in each block are then calculated. The position and the orientation of the point are rotated to the orientation of the keypoint so that the descriptor can be robust to image rotation. Finally, the gradient magnitude is projected to the histogram with 8 bins for the orientation. Figure 3 shows the process of this stage.

Recently, another methods using wavelet transform are studied to detect interest points. E. Loupias et al. proposed a salient point detector based on wavelet transform to detect relevant points with high global variations[13]. D. W. Lin et al. proposed a salient region detector based on Daubechies (9, 7) filter[12].

III. The Proposed Detector

This section describes the main process of the proposed detector. For detecting the interest points,

we form a high frequency image by using the Haar wavelet transform. The high frequency image is subsequently used to form an integral image for fast computation. The local variance of the original image is then evaluated by the average box filter, and finally we locate the interest points.

1. Formation of the high frequency image by using the Haar wavelet transform

Wavelet technology provides sophisticated mathematical and statistical routines for analyzing signals and very large data sets. In recent years, the wavelet technology has been applied increasingly widely in the field of image processing[25~26, 28]. Because the Haar wavelet forms an orthogonal basis, it provides a non-redundant representation of an image. Furthermore, it is thought to be easier to implement the Haar wavelet than other wavelet functions, and it can be executed with less computation cost. With the aim of exploiting these advantages, we decompose an original image using the Haar wavelet transform and obtain the high frequency information from the image. Different levels of decomposition can be performed to the input image to yield different scales of the image. The input image can be decomposed into four sub-band images, as shown in Figure 4: LL image denotes the approximation of the input image; HL image denotes the high frequency information of the horizontal direction; LH denotes the high frequency information of the vertical direction; and HH denotes the high frequency information of the diagonal direction.

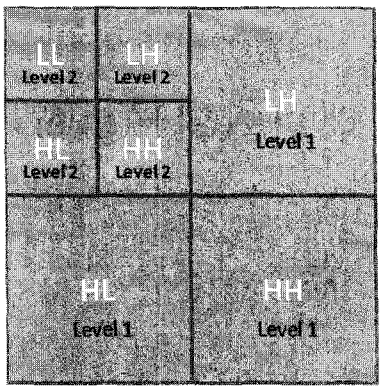

그림 4. Haar 웨이블릿을 이용한 영상 분할
Fig. 4. Decomposition of the image by using the Haar wavelet.

The HL, LH, and HH images denote the local variance information of the image in different directions. Since the variance stems from jitter of the proximity pixels, it offers more distinctive information of the local region of an image and is thus robust to illumination change. Therefore, we can fuse these three images to form a high frequency image and use the average box filter to evaluate the local variance of the original image. The fusion of these three images is a simple process of summing up the pixel values of the images point by point. Finally, we normalize the summation image with the gray scale in a range from 0 to 255.

2. Formation of the integral image

The integral image is very useful for fast computation when box filters are applied to the image[2, 25]. The integral image at location (x, y) contains the sum of the pixels above and to the left of x, y; it can be calculated as follows:

$$I(x,y)=\sum_{x'\le x,y'\le y} i(x',y') \tag{1}$$

where $I(x, y)$ is the integral image at the location (x, y) and $i(x', y')$ is the original image at the location (x', y').

Thus, by using an integral image, we can obtain rapidly a summation of a rectangular region in the image because only three simple computation steps are needed. Figure 5 shows the process of calculating the sum of a rectangular region in the integral image.

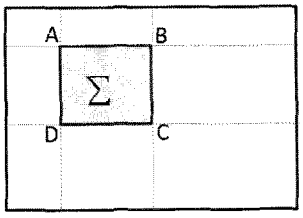

The summation of the rectangular region ABCD is:

$$\sum = A + C - B - D$$

그림 5. 적분 영상의 응용
Fig. 5. Application of the integral image.

3. Average box filter operation

Our purpose is to detect interest points that represent the regions with local highest variance information among their neighbor regions. Thus, after obtaining the integral image, we apply average box filters with increasing sizes to evaluate the local variance information. The convolution of the filter and the high frequency image results in a smoothed image. Further, it is obvious that the value of each point in the smoothed image represents the variance information of the region surrounding the point and the size of region is the same as that of the filter. As shown in Figure 6, the value of the black point is the average of the rectangle, and thus we use it to represent the variance information of the rectangular region.

Since the function of the average box filter is to calculate the average value of the points within a rectangular region, instead of using the high frequency image, we use the integral image to obtain the average value for fast computation. Different sizes of average box filters are applied to build the image pyramid, as shown in Figure 1.

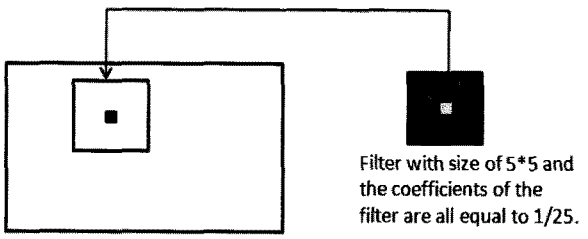

그림 6. 평균 박스 필터 연산
Fig. 6. The average box filter operation.

4. Interest point location

After building the image pyramid by using the Haar wavelet transform and the average box filter, the pixel values in the smoothed image represent the local variance information of the original image: the smaller the point value is, the lower the variance is. Thus, the small value points are pruned by a threshold and finally we obtain the candidate points.

In this paper, we propose using the average value and the standard deviation of the high frequency image to set an adaptive threshold. Suppose that the average value of the high frequency image I in octave n is A_g and the standard deviation of image I is *Sigma*; the threshold T for octave n can then be set as follows:

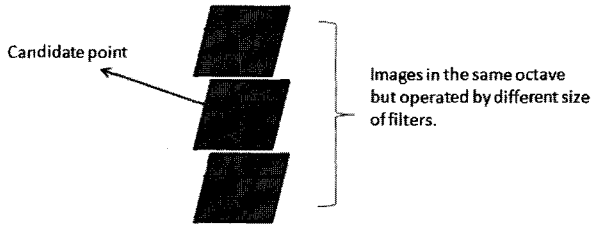

그림 7. 최대점 결정
Fig. 7. Location of maximum point.

$$T = A_g + Sigma \tag{2}$$

In the same octave of the image pyramid, the points whose values are greater than the threshold T are selected as candidate points. The candidate point is then used for comparing with its 26 neighbors, as shown in Figure 7. If its value is the maximum among the points, we determine it to be an interest point.

Ⅳ. Experimental Results

To evaluate the performance of the proposed method, we compare the repeatability, the number of interest points, the execution time and the matching accuracy with those of the DoG detector and the Harris corner detector. Table 1 describes the experimental environment.

표 1. 실험 환경
Table 1. The experimental environment.

Operation system	windows xp
CPU	Dual core(TM) 2.4 GHz
Memory	2 GB
Programming tool	VC++ 6.0 and OpenCV

1. The parameters

In order to build an image pyramid and evaluate the local variance of the image in the image pyramid, we must determine the size of the box filter, the number of octaves, and the number of images in each octave. In this paper, the size of the filter S of an image $I(I=0,1,2...)$ in octave $O(O=0,1,2\cdots)$ is determine as follows:

$$S = Init + n \times O + m \times I \tag{3}$$

where *Init* is the initial size of the filter and is set to 5, and n and m are increasing factors and are set to 2, respectively. The number of octaves is determined by the size of the filter and the size of the image. We increase the number of octaves until the largest size of the filter is larger than the size of the image in the same octave. The number of images in each octave is set to 7 by executing experiments that achieve highest repeatability. These parameters are used for the following experiments.

2. The repeatability

The repeatability is calculated by taking into account the point location with the type of transform, such as illumination, image size, and rotation. Two points in different images are considered as corresponding if their relative location satisfies the following formula:

$$\| P_1, A \cdot P_2 \| \leq T \tag{4}$$

where P_1 and P_2 are the points in both images, A is the transform action and T is a threshold that is set to 2 in the following experiments. Thus, the repeatability rate between two images is the ratio of the number of corresponding points and the number of detected points.

To evaluate the repeatability, we utilize the object image dataset collected by the Computer Vision Laboratory of the Department of Information Technology and Electrical Engineering in Zurich, Switzerland[34]. There are 51 objects in the dataset and all the objects in the images are with white background. We select 20 images (20 different objects) from the dataset randomly and change the illumination and size, and rotate the image with different degrees artificially for testing the repeatability. First, we changed the illumination of the images by the factor of -40, -20, 10, 20, 30, and 40. Second, we change the size of the original images by the factor of 0.4, 0.8, 1.2, 1.6, 2.0 and 2.4. Finally, the original images are rotated with degrees of 10, 20, 30, 45, and 60. Note that the size of the original image is 320 by 240.

Figures 8 and 9 show the repeatability and time consumption of the proposed detector, the Harris corner detector, and the DoG detector with the rotation transform. It is found that the proposed detector (HWFD) achieves higher repeatability than those of the Harris corner detector and DoG detector, respectively, in most of the cases. Since the Harris corner detector does not build an image pyramid, it achieves the fastest speed. Because the proposed detector applies the integral image technique, it performs almost as fast as the Harris corner detector even though an image pyramid is built.

Figures 10 and 11 show the repeatability and time consumption under illumination change. It is observed that the proposed detector achieves the highest repeatability. Due to requiring less computation, the Harris corner detector provides the fastest performance. The proposed detector also performs

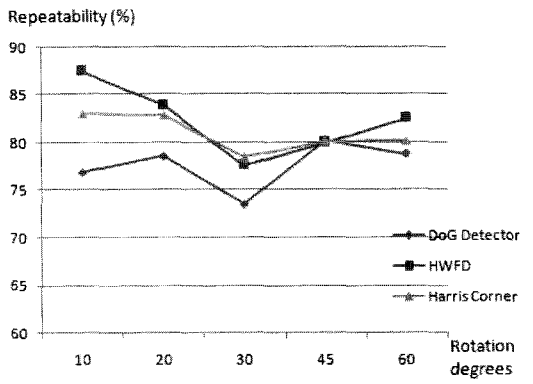

그림 8. 회전 변환에 따른 반복도
Fig. 8. Repeatability in the case of rotation transforms.

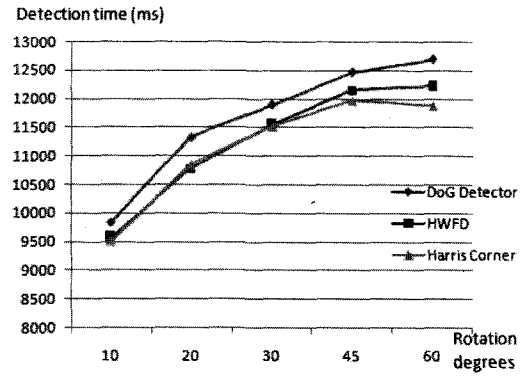

그림 9. 회전 변환에 따른 소요 시간
Fig. 9. Time consumption in the case of rotation transforms.

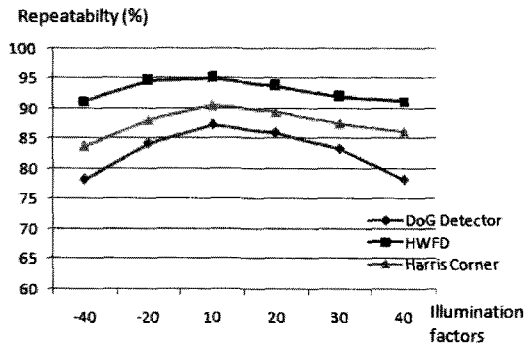

그림 10. 명암도 변화에 따른 반복도
Fig. 10. Repeatability in the case of illumination change.

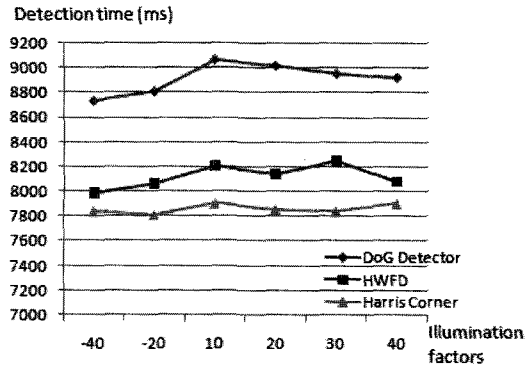

그림 11. 명암도 변화에 따른 소요 시간
Fig. 11. Time consumption in the case of illumination change.

faster than the DoG detector.

As we can observe from Figures 12 and 13, the proposed detector also achieves higher repeatability than those of the DoG detector and Harris corner detector, respectively, in most of the cases when image size is changed. Also, it is found that the time

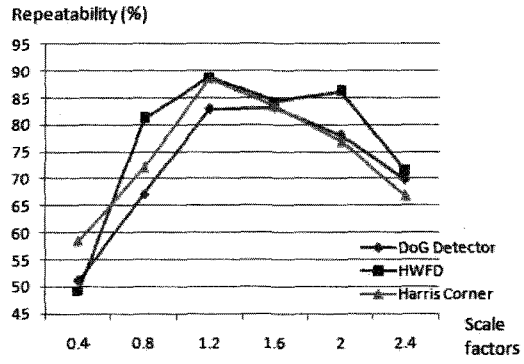

그림 12. 영상 크기 변화에 따른 반복도
Fig. 12. Repeatability in the case of change of the image size.

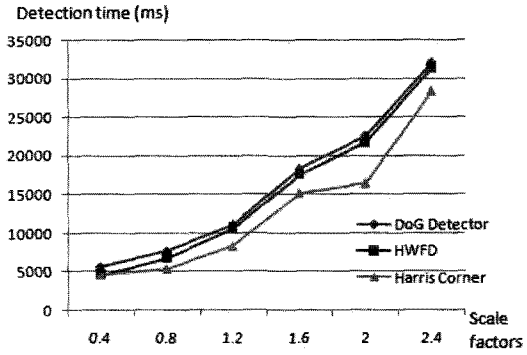

그림 13. 영상 크기 변화에 다른 소요 시간
Fig. 13. Time consumption in the case of change of the image size.

consumption of the proposed detector is moderate and the Harris corner detector consumes the least time.

3. The matching accuracy

After we locate the interest points in the image by using the proposed detector, the Harris corner detector, and the DoG detector, we calculate the orientation of the point and form a descriptor for each interest point, as SIFT[15] does. To verify that the interest points detected by the proposed detector have higher local information and are more distinctive, an application for matching real-world scenes is executed and the matching results of the proposed method are compared with those of the DoG detector and the Harris corner detector, respectively. We use a dataset[35] that includes household items with different sizes, viewpoints, illumination, and rotation with different degrees for the matching

experiment. This dataset was utilized to evaluate the performance of PCA-SIFT[10]. The size of image in the dataset is 640 by 480.

The distance of two points is calculated by using the Euclidean distance:

$$D_{ij} = \| F_i - F_j \| = \sqrt{\sum_{k=1}^{N} (F_{i,k} - F_{j,k})^2} \quad (5)$$

where D_{ij} is the distance of two interest points P_i and P_j. F_i and F_j are the features of P_i and P_j, respectively. N is the dimension of the feature.

For a single point P_i in the image I, we calculate the distance values between P_i and all the points in the other image J. If the closest distance is smaller than a threshold T (280 for the proposed method, 250 for the Harris corner detector and 260 for the DoG detector which give the best matching result for each method, respectively), we determine that the image pair I and J is matched. To assess the matching accuracy, we randomly select one of the images from the dataset and use it to match the others. For a selected image, we can obtain the number of matching pairs with the others, as shown in Figure 14.

As shown in Figure 14, I_s is the selected image while I_1, I_2, I_3,$\cdots$,I_n are the other images in the dataset. N_1, N_2, N_3,$\cdots$,N_n are the corresponding matching pairs between the image I_s and the images I_1, I_2, I_3,$\cdots$,I_n. We then rank I_1, I_2, I_3,$\cdots$,I_n in the order of the number of matching pairs(N_1, N_2, N_3,$\cdots$,N_n) from the greatest to the smallest. If the corresponding images are ranked in the top positions,

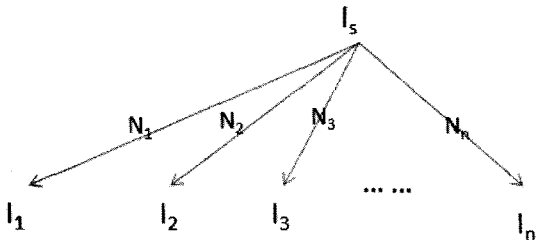

그림 14. 매칭 과정
Fig. 14. The matching process.

표 2. 매칭 결과
Table 2. The matching results.

Algorithm	Matching accuracy	Point number	Average time consumption
DoG	51.67 %	40219	2474 ms
HWFD	60 %	23288	1415 ms
Harris	20 %	27729	1694 ms

we consider the matching to be correct. By repeating the process of selecting each image from the set and matching it to the other images, we obtain the total number of correct matches, *correctN*. Suppose that the total number of similar images corresponding to the selected images in the image set is *similarN* .The matching accuracy can then be defined as follows:

$$accuracy = \frac{correctN}{similarN} \quad (6)$$

The matching results are listed in Table 2. Since the proposed detector detects interest points that represent the local regions whose variance is the highest based on a comparison with their neighbors, the proposed method achieves higher matching accuracy than those of the DoG detector and the Harris corner detector, respectively while having the lowest number of interest points. Since fewer points are used, the proposed detector obtains the fastest matching speed.

IV. Conclusion

This paper proposes a new feature detector based on the Haar wavelet transform and average box filter. We apply the Haar wavelet transform to decompose the input image so as to obtain the local variance information of the original image. Aiming at finding interest points to represent the local regions whose variance information is the highest when compared to their neighbors, average box filters with different size are used to evaluate the local variance of the regions. By building an image pyramid, we detect interest points in each octave. For fast

detection, the integral image technique is also applied. Due to the properties of the Haar wavelet transform and the usage of the box filter, the proposed detector is robust to illumination change, image size change, and rotation. Since the detector detects more distinctive interest points and reduces the number of interest points, it yields improved efficiency and matching accuracy when applied to image matching.

References

[1] S. Allaire, J. J. Kim, S. L. Breen, D. A. Jaffray, V. Pekar, "Full orientation invariance and improved feature selectivity of 3D SIFT with application to medical image analysis," IEEE Computer Society Conference on Computer Vision and Pattern Recognition Workshops, pp.1-8, 2008.

[2] H. Bay, A. Ess, T. Tuytelaars, and L. V. Gool, "Speeded-Up Robust Features", Computer Vision and Image Understanding, Vol.110, pp.346 - 359, 2008.

[3] M. Bicego, A. Lagorio, E. Grossoa and M. Tistarelli, "On the use of SIFT features for face authentication," In: Proceedings of the Conference on Computer Vision and Pattern Recognition Workshop, pp.17-22, 2006.

[4] J. Chen, J. Tian, "Real-time multi-modal rigid registration based on a novel symmetric-SIFT descriptor," Process in Natural Science, Vol.19, pp.643-651, 2009.

[5] G. Csurka, C. B. Dance, L. Fan, J. Willamowski, and C. Bray, "Visual categorization with bags of keypoints," In: Proceedings of Workshop on Statistical Learning in Computer Vision, 2004.

[6] G. G. Ding, Q. H. Dai, W. L. Xu and F. Yang, "Affine-Invariant Image Retrieval Based on Wavelet Interest Points," In: Proceedings of Seventh IEEE Multimedia Signal Processing Workshop, pp.1-4, 2005.

[7] K. Gao, S. X. Lin, Y. D. Zhang, S. Tang, H. M. Ren, "Attention Model Based SIFT Keypoints Filtration for Image Retrieval," In: Proceedings of IEEE/ACIS International Conference on Computer and Information Science, pp.191-196, May 2008.

[8] C. Harris, M. Stephens, "A combined corner and edge detector," In: Proceedings of the Fourth Alvey Vision Conference, pp.147 - 151, 1988.

[9] X. L. Hu, Y. C. Tang, and Z. H. Zhang, "Video Object Matching Based on SIFT Algorithm," In: Proceedings of IEEE International Neural Networks and Signal Processing Conference, pp.412-415, 2008.

[10] Y. Ke, R. Sukthankar, "PCA-SIFT: A More Distinctive Representation for Local Image Descriptors," In: Proceedings of Intl. Conference on Computer Vision and Pattern Recognition, pp.506-513, 2004.

[11] D. H. Kim, J. W. Song, J. H. Lee, and B. G. Choi, "Support Vector Machine Learning for Region-Based Image Retrieval With Relevance Feedback," ETRI Journal, Vol. 29, No.5, 2007.

[12] D. W. Lin, S. H. Yang, "Wavelet-Based Salient Region Extraction," on the conference of Advances in Multimedia Information Processing, pp.389-392, 2007.

[13] E. Loupias N. Sebe S. Bres J. M. Jolion, "Wavelet-Based Salient Points for Image Retrieval," In: Proceedings of Intl. Conference on Image Processing, pp.518-521, 2000.

[14] D. Lowe, "Object recognition from local scale-invariant features," In: Proceedings of the seventh IEEE International Computer Vision, Vol.2, pp.1150-1157, 1999.

[15] D. Lowe, "Distinctive image features from scale-invariant keypoints," International Journal of Computer Vision, Vol.60, pp. 91-110, 2004.

[16] H. L. Luo, H. Wei, Y. Ren, "Combining Different Interest Piont Detectors for Object Categorization," In: Proceedings of Intl. Conference on Machine Learning and Cybernetics, pp.34-38, 2009.

[17] J. Matas, J. Burianek, and J. Kittler, "Object recognition using the invariant pixelset signature," In: Proceedings of Eleventh British Machine Vision Conference, pp. 606-615, 2000.

[18] K. Mikolajczyk, and C. Schmid, "Indexing based on scale invariant interest points," In: Proceedings of Eighth IEEE Intl.Computer Vision Conference, Vol. 1, pp. 525 - 531, 2001.

[19] C. Schmid and R. Mohr, "Local grayvalue invariants for image retrieval," IEEE Transactions on Pattern Analysis and Machine Intelligence, Vol. 19, pp.530 - 535, 1997.

[20] S. Se, D. Lowe, J. Little, "Vision-based mobile robot localization and mapping using scale-invariant features," In: Proceedings of IEEE Intl.Conference on Robotics and Automation, vol.2, pp.2051-2058, 2001.

[21] X. Y. Song, H. K. Lee, H. Q. Cho, "A Sensor Fusion Method for Mobile Robot Navigation," In: Proceedings of Intl. Joint Conference on SICE_ICASE, pp.5310-5316, Oct. 2006.
[22] Q. Tu, Y. P. Xu, M. L. Zhou, "Robust vehicle tracking based on Scale Invariant Feature Transform," In: Proceedings of Intl. Conference on Information and Automation, pp.86-90, Jun. 2008.
[23] T. Tuytelaars, L.V. Gool, L. D'haene, and R. Koch, "Matching of affinely invariant regions for visual servoing," In: Proceedings of IEEE Intl. Conference on Robotics and Automation, Vol.2, pp.1601-1606, 1999.
[24] M. Urschler, J. Bauer, H. Ditt, and H. Bischof, "SIFT and Shape Context for Feature-Based Nonlinear Registration of Thoracic CT Images," In: Proceedings of Computer Vision Approaches to Medical Image Analysis, pp.73-84, 2006.
[25] P. Viola, and M. Jones, "Rapid Object Detection using a Boost Cascade of Simple Features," In: Proceedings of Computer Vision and Pattern Recognition, Vol. 1, pp. 511 - 518, 2001.
[26] X. Wang, "Moving Window-Based Double Haar Wavelet Transform for Image Processing," IEEE Transactions on Image Processing, Vol. 15, pp. 2771-2779, 2006.
[27] Z. Z. Wang, K. B. Jia, P. Y. Liu, "A Novel Image Retrieval Algorithm Based on ROI by Using SIFT Feature Matching," In: Proceedings of Intl. Conference on MultiMedia and Information Technology, pp.338-341, Dec. 2008.
[28] X. Z. Wen, H. Yuan, C. Y.Yang, C. Y. Song, B. Duan and H. Zhao, "Improved Haar Wavelet Feature Extraction Approaches for Vehicle Detection," In: Proceedings of IEEE Intelligent Transportation Systems Conference, pp. 1050-1053, 2007.
[29] Y. Y. Wu, Y. Q. Wu, "Shape-Based Image Retrieval Using Combining Global and Local Shape Features," In: Proceedings of 2nd Intl. Congress on Image and Signal Processing, pp.1-5, Oct. 2009.
[30] H. Zhou, Y. Yuan, and C. Shi, "Object tracking using SIFT features and Mean Shift," Computer Vision and Image Understanding, 2008.
[31] H. Zhoua,Y. Yuanb and C. Shic, "Object tracking using SIFT features and mean shift," Computer Vision and Image Understanding, Vol.113, pp.345-352, 2009.
[32] 이덕운, 남우현, 나종범, "진단 및 치료를 위한 3차원 의료 영상의 응용", 대한전자공학회 전자공학회지, 제35권, 제4호, pp. 67-75, 2008년 4월
[33] 황운주, 박성욱, 박종관, 박종욱, "지문 영상의 분해 및 합성에 의한 주름선 검출방법", 대한전자공학회, 전자공학회논문지-CI, 제44권, 제3호, pp. 90-97, 2007년 5월
[34] http://www.vision.ee.ethz.ch/
[35] http://www.cs.cmu.edu/~yke/pcasift/objects.tgz

저 자 소 개

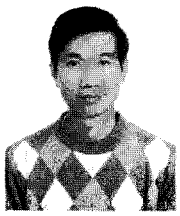

팽 소 호(학생회원)
2005년 광동공업대학 정보공학 학사 졸업.
2007년 광동공업대학 정보공학 석사 졸업.
2008년~현재 인하대학교 전자공학과 박사과정 재학.
<주관심분야 : 의료영상처리, 컴퓨터비전>

뮤 잠 멜(학생회원)
2009년 인하대학교 전자공학과 학사 졸업.
2009년~현재 인하대학교 전자공학과 석사과정 재학.
<주관심분야 : 영상처리, 멀티미디어, 임베디드 시스템>

김 현 수(학생회원)
2008년 인하대학교 컴퓨터공학과 학사 졸업.
2008년~현재 인하대학교 전자공학과 석사과정 재학.
<주관심분야 : 인공지능, 멀티미디어, 모바일 플랫폼>

김 덕 환(정회원)-교신저자
2003년 한국 과학 기술원 컴퓨터공학 박사.
2006년~현재 인하대학교 전자공학부 부교수
<주관심분야 : 시각정보처리, 멀티미디어시스템,임베디드 시스템>